Acknowledgement is made to the Department of Science and Technology and the Department of Atomic Energy, Government of India, for financial support.

Registry No. $MoO_2(PhH)_2$, 76582-00-8; $MoO_2(PhMe)_2$, 84927-86-6; $MoO_2(PhOMe)_2$, 84927-87-7; $MoO_2(PhCl)_2$, 84927-88-8; $MoO_2(PhNO_2)_2$, 84927-89-9; $MoO_2(MeH)_2$, 84927-90-2; $MoO_2(MeMe)_2$, 84927-91-3; $MoO_2(MeOMe)_2$, 84927-92-4; $MoO_2(MeCl)_2$, 84927-93-5; $MoO_2(MeNO_2)_2$, 84927-94-6; $MoO_2(HH)_2$, 67315-41-7; $MoO_2(HMe)_2$, 84927-95-7; $MoO_2(HOMe)_2$, 84927-96-8; $MoO_2(HCl)_2$, 84985-80-8; $MoO_2(HNO_2)$, 84985-81-9; PhNHOH, 100-65-2.

Supplementary Material Available: A listing of analytical data (1 page). Ordering information is given on any current masthead page.

Contribution from the Departments of Chemistry, Texas A&M University, College Station, Texas, and University of Kentucky, Lexington, Kentucky 40506

Reaction of Halide Ions with Tetrakis(μ-trifluoroacetato)dimolybdenum(II): Crystal Structures of $(N\text{-}n\text{-}Bu_4)_2[Mo_2(O_2CCF_3)_4X_2]$ (X = Br, I) and $(N\text{-}n\text{-}Bu_4)_2[Mo_2(O_2CCF_3)_2Br_4]$

F. ALBERT COTTON and PHILLIP E. FANWICK*

Received August 18, 1982

The reaction of $Mo_2(O_2CCF_3)_4$ with tetra-*n*-butylammonium halides is reported. In acetone, orange solutions were obtained, which upon evaporation yielded the axial diadducts $[Mo_2(O_2CCF_3)_4X_2]^{2-}$ (X = Br, I). The bromide compound crystallized in the space group $P2_1/n$ with $a = 16.411$ (6) Å, $b = 14.660$ (7) Å, $c = 12.313$ (4) Å, $\beta = 96.29$ (3)°, $V = 2944$ (4) Å^3, and $Z = 2$ while the iodo compound crystallized in the space group $P\bar{1}$ with $a = 13.478$ (2) Å, $b = 17.013$ (2) Å, $c = 12.638$ (2) Å, $\alpha = 92.64$ (1)°, $\beta = 92.52$ (1)°, $\gamma = 78.48$ (1)°, $V = 2834$ (2) Å^3, and $Z = 2$. Concentrated solutions in benzene formed a gel, which upon addition of acetone yielded crystals of $(N\text{-}n\text{-}Bu_4)_2[Mo_2(O_2CCF_3)_2Br_4]$, with a centrosymmetric trans anion. This compound crystallized in the space group $P2_1/n$ with $a = 13.379$ (1) Å, $b = 15.793$ (5) Å, $c = 13.712$ (6) Å, $\beta = 101.17$ (2)°, $V = 2842$ (3) Å^3, and $Z = 2$. The metal-metal distance in this compound, 2.098 (1) Å, was quite comparable to that in $Mo_2(O_2CCF_3)_4$ while, in the diadducts, the Mo–Mo distances, 2.134 (2) to 2.140 (2) Å, were significantly longer. The axial Mo–X distances in the diadducts were longer than when these ligands are coordinated in the equatorial plane.

Introduction

Since the discovery of dinuclear quadruply bonded molecules, the tetracarboxylate compounds have formed a cornerstone in their chemistry. The metals chromium, molybdenum, tungsten, technetium, and rhenium all form examples.[1] However, there has always been one notable difference between the compounds of molybdenum, and perhaps tungsten, and those of the other metals. In the compounds of molybdenum each metal atom is four-coordinate while the other metal atoms tend to bond to five ligands. The extra ligands occupy sites along the metal–metal bond and will be referred to as axial ligands. For technetium and rhenium the presence of axial ligands is easily explained. The M^{3+} dimers of these metals are cations. The inclusion of two anionic ligands (usually halide ions from the precursor $[M_2X_8]^{2-}$ ions) results in a neutral complex. In the case of chromium, it is not as clear why these extra ligands are required. However, the effects of the axial ligands are important, resulting in unusually long Cr–Cr bond distances. For example, the metal–metal distance in $Cr_2(O_2CCH_3)_4(H_2O)_2$ is 2.362 (1) Å,[2] which is considerably longer than the 2.0934 (8)Å observed in $Mo_2(O_2CCH_3)_4$.[3]

When initially prepared, the dimolybdenum tetracarboxylates did not appear to have any tendency to coordinate to axial ligands. Neither the acetate nor the benzoate compounds displayed axial coordination. However, there are weak intermolecular interactions between the coordinated oxygen atoms and the axial positions of an adjacent molecule, which have important effects, at least with respect to the solid-state spectrum.[3-4] On the other hand, $Mo_2(O_2CCF_3)_4$ displays a greater tendency to axial coordination. It was initially noted that crystals grown from solvents with donor atoms always contained molecules of solvation.[5] Crystals of the unsolvated complex were obtained only by sublimation. In addition, the bis(pyridine) adduct of $Mo_2(O_2CCF_3)_4$ was later structurally characterized.[6] The Mo–Mo bond distance was found to be lengthened by 0.039 Å in this adduct.

In 1975, Garner and Senior reported that reacting $Mo_2(O_2CCF_3)_4$ with 1 or 2 equiv of tetraethylammonium bromide or iodide resulted in the formation of the mono- and diadducts.[7] Interestingly, when the corresponding chloride was used, the only products obtained were the monoadduct or $[Et_4N]_2[Mo_2(O_2CCF_3)_3Cl_3]$, where two chloride ions have displaced a trifluoroacetate. From the Raman spectra, these authors concluded that the Mo–Mo bonds in these axial adducts were weaker than those in the starting dimer. For this reason, it was felt that these complexes should be characterized by X-ray crystallography. In this paper we report the crystal structures of the analogous tetra-*n*-butylammonium bromide and iodide diadducts. When the bromide solutions were used, the compound $(N\text{-}n\text{-}Bu_4)_2[Mo_2(O_2CCF_3)_2Br_4]$ was also isolated and structurally characterized. In addition, we discuss the solution spectrum of $[Mo_2(O_2CCF_3)_4]$ in the presence of bromide ion. In a future paper we will report on the low-temperature polarized crystal spectra of the dibromo and diiodo adducts.

Experimental Section

All solvents used were dried by using literature methods and distilled under nitrogen prior to use. All reactions and evaporations were done under dry nitrogen.

Preparation of $(N\text{-}n\text{-}Bu_4)_2[Mo_2(O_2CCF_3)_4Br_2]$. In a typical reaction 0.5 g of $Mo_2(O_2CCF_3)_4$, which was prepared by the literature procedure,[5] and 0.5 g of $(N\text{-}n\text{-}Bu_4)Br$ were refluxed in benzene for 4–5

---

* To whom correspondence should be addressed at the University of Kentucky.

(1) Cotton, F. A.; Walton, R. A. "Multiple Bonds Between Metal Atoms"; Wiley: New York, 1982.
(2) Cotton, F. A.; DeBoer, B. G.; LaPrade, M. D.; Papal, J. R.; Ucko, D. A. *Acta Crystallogr., Sect. B* **1971**, *B27*, 1664.
(3) Cotton, F. A.; Mester, Z. C.; Webb, T. R. *Acta Crystallogr., Sect. B* **1974**, *B30*, 2768.
(4) Martin, D. S.; Newman, R. A.; Fanwick, P. E. *Inorg. Chem.* **1982**, *21*, 3400.
(5) Cotton, F. A.; Norman, J. G., Jr. *J. Coord. Chem.* **1971**, *1*, 161.
(6) Cotton, F. A.; Norman, J. G., Jr. *J. Am. Chem. Soc.* **1972**, *94*, 5967.
(7) Garner, C. D.; Senior, R. G. *J. Chem. Soc., Dalton Trans.* **1975**, 1171.

0020-1669/83/1322-1327$01.50/0

Table I. Crystallographic Data

	$(N\text{-}n\text{-}Bu_4)_2$-$[Mo_2(O_2$-$CCF_3)_4Br_2]$	$(N\text{-}n\text{-}Bu_4)_2$-$[Mo_2(O_2$-$CCF_3)_4I_2]$	$(N\text{-}n\text{-}Bu_4)_2$-$[Mo_2(O_2$-$CCF_3)_2Br_4]$
a, Å	16.411 (6)	13.478 (2)	13.379 (1)
b, Å	14.660 (7)	17.013 (2)	15.793 (5)
c, Å	12.313 (4)	12.638 (2)	13.712 (6)
α, deg	90	92.64 (1)	90
β, deg	96.29 (3)	92.52 (1)	101.17 (2)
γ, deg	90	78.48 (1)	90
V, $Å^3$	2944 (4)	2834 (2)	2842 (3)
Z	2	2	2
space group	$P2_1/n$	$P\bar{1}$	$P2_1/n$
density, g cm^{-3}	1.454	1.621	1.428
abs coeff, cm^{-1}	19.41	16.30	34.67
formula wt	1288.71	1382.70	1222.49
cryst size, mm	0.4 × 0.4 × 0.3	0.5 × 0.4 × 0.1	0.4 × 0.4 × 0.4
range of 2θ, deg	0–45	0–45	0–45
no. of unique data	4191	7407	3898
data with $I > 3\sigma(I)$	1558	5517	2533
R_1	0.065	0.054	0.050
R_2	0.083	0.070	0.068

h. The yellow precipitate formed was filtered in air and washed with pentane. After being washed, the powder was yellow-orange. Crystals suitable for X-ray studies were obtained by slowly evaporating a solution of this powder dissolved in acetone. The resulting crystals displayed only slight decomposition after standing in air for over 1 week.

Preparation of $(N\text{-}n\text{-}Bu_4)_2[Mo_2(O_2CCF_3)_4I_2]$. Crystals of this compound were prepared by dissolving 0.5 g of $Mo_2(O_2CCF_3)_4$ and 2 equiv of $(N\text{-}n\text{-}Bu_4)I$ in acetone and evaporating the solvent. The crystals have the same appearance and reactivity as the analogous bromide complex.

Preparation of $(N\text{-}n\text{-}Bu_4)_2[Mo_2(O_2CCF_3)_2Br_4]$. $Mo_2(O_2CCF_3)_4$ and 4 equiv of $(N\text{-}n\text{-}Bu_4)Br$ were dissolved in as small a volume of benzene as possible. Upon standing 10–14 days, the solution had become a yellow gel. At this point, ~10 mL of acetone was added. The resulting mixture consisted of two phases, which separated even after agitation. After about 20–30 days, large orange crystals of $(N\text{-}n\text{-}Bu_4)_2[Mo_2(O_2CCF_3)_2Br_4]$ were observed growing at the interface of the two phases. One of these crystals was cleaved with a razor blade and used for the structural study. The crystals were very air stable.

Crystallographic Study of $(N\text{-}n\text{-}Bu_4)_2[Mo_2(O_2CCF_3)_4Br_2]$. A crystal prepared as above was cemented to a glass fiber and mounted on a Syntex $P\bar{1}$ four-circle automated diffractometer. Lattice parameters were obtained by a least-squares fit for 15 strong reflections with 20° < 2θ < 30°. Data collection and refinement procedures used were as previously reported.[8,9] The crystallographic data are reported in Table I. The systematic absences $0k0$, $k = 2n + 1$, and $h0l$, $h + l = 2n + 1$, uniquely identified the space group as $P2_1/n$.

The patterson map did not prove tractable because of the similarity in intensity between the Mo–Mo and Mo–Br vectors and the large number of additional parallel vectors. Attempts to phase the data using MULTAN were unsuccessfuly because the distribution of the intense *E*'s was strongly indicative of *c* centering. The renormalization of the *E*'s by class in order to overcome the pseudo *c* centering did not lead to a solution. As a last attempt, the symmetry of the cell was given as the nonexistent space group $C2_1/n$ and the direct-methods programs were rerun. From the resulting *E*-map, positions for the Mo and Br atoms were obtained and transferred to a cell with the observed $P2_1/n$ symmetry. Least-squares and Fourier techniques were then used to refine the structure to convergence. The function minimized was $\sum w(|F_o| - |F_c|)^2$, where the weight was given by $w = 1/\sigma^2(F_o^2)$. The value of the *p* factor used in the calculation of $\sigma(F_o)$ was 0.07.[10]

Data reduction and structural refinement were carried out by using the Enraf-Nonius Structure Determination Package on the PDP 11/45 computer at the Molecular Structure Corp. An empirical absorption correction was applied to the data. The final difference Fourier map displayed no peak with intensity greater than 0.6 e/$Å^3$. For this structure and the others reported the hydrogen atoms of the tetrabutylammonium ion were not observed nor refined.

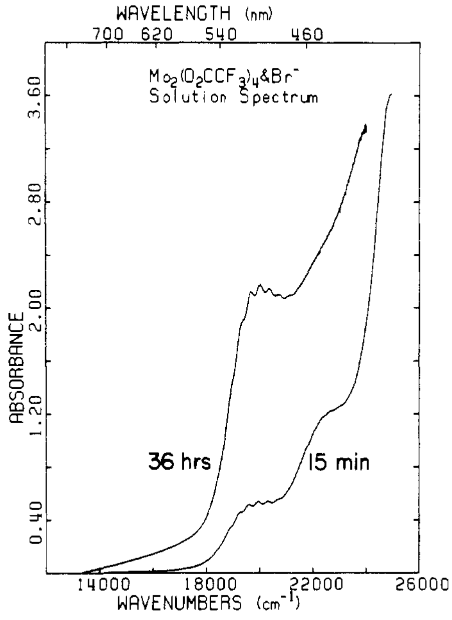

Figure 1. Solution spectrum of 5.0×10^{-3} M $Mo_2(O_2CCF_3)_4$ and 1.0×10^{-1} M Br^- in acetone.

Crystallographic Study of $(N\text{-}n\text{-}Bu_4)_2[Mo_2(O_2CCF_3)_4I_2]$. A crystal prepared as above was mounted on an Enraf-Nonius CAD-4 diffractometer. Lattice parameters were obtained by least-squares fit to 25 random reflections with 22° < 2θ < 32°. The crystallographic data are given in Table I. The structure was refined on the IBM 370/165 computer at the University of Kentucky Computing Center by using procedures previously described.[11] The value of the *p* factor was 0.01. The initial positions for the Mo and I atoms were obtained from *E* maps generated by MULTAN77. Both the *E* maps and the Patterson map indicated that there were two independent molecules in the cell, with each residing on an inversion center. An empirical absorption correction using Flack's CAMEL JOCKEY WITH THREE HUMPS was applied.[12] Refinement converged to the residuals reported. The largest peak in the final difference Fourier was 0.3 e/$Å^3$.

Crystallographic Study of $(N\text{-}n\text{-}Bu_4)_2[Mo_2(O_2CCF_3)_2Br_4]$. Data were collected, and the cell was determined on an Enraf-Nonius CAD-4 automated diffractometer. The unit cell was based on the least-squares fit for 25 random reflections with 18° < 2θ 32°. While the half-widths of the peaks were quite acceptable, the backgrounds were very high. In order to obtain as much statistically meaningful data as possible, a large crystal was used. Procedures used with the CAD-4 have been described previously.[13] Again refinement was carried out by using the Enraf-Nonius Structure Determination Package. The initial positions were obtained from *E* maps produced by MULTAN. Refinement was carried out as before. An empirical absorption correction was applied to the data. The final difference Fourier maps displayed no peaks greater than 0.3 e/$Å^3$.

Electronic Spectrum. The solution spectrum was recorded on a Cary 17-D spectrophotometer interfaced to a NOVA 1200 computer as previously described.[14] The spectrum was plotted on a VERSATEC plotter.

Results and Discussion

Reactions. When bromide or iodide ions were added to a solution of $[Mo_2(O_2CCF_3)_4]$, there was an immediate color change from yellow to orange. While there was no obvious color change after that, the spectra of these solutions showed a change with time. The solution spectrum in acetone of 5.0

---

(8) Cotton, F. A.; Frenz, B. A.; Deganello, G.; Shaver, A. *J. Organomet. Chem.* **1973**, *50*, 227.

(9) Adams, R. D.; Collins, D. M.; Cotton, F. A. *J. Am. Chem. Soc.* **1974**, *96*, 749.

(10) Corfield, P. W. R.; Doedens, R. J.; Ibers, J. A. *Inorg. Chem.* **1967**, *6*, 197.

(11) Fanwick, P. E.; Huckaby, J. L. *Inorg. Chem.* **1982**, *21*, 3067.

(12) Flack, H. D. *Acta Crystallogr. Sect. A* **1977**, *A33*, 890.

(13) Bino, A.; Cotton, F. A.; Fanwick, P. E. *Inorg. Chem.* **1970**, *9*, 351.

(14) Cotton, F. A.; Fanwick, P. E. *J. Am. Chem. Soc.* **1979**, *101*, 5252.

Table II. Vibrational Structure Observed in the Solution Spectrum of $\mathrm{Mo_2(O_2CCF_3)_4}$ and $\mathrm{Br^-}$ [a]

λ, nm	$\tilde{\nu}$, cm^{-1}	$\Delta\tilde{\nu}$, cm^{-1}	λ, nm	$\tilde{\nu}$, cm^{-1}	$\Delta\tilde{\nu}$, cm^{-1}
523.6	19 098		487.5	20 513	
514.1	19 451	353	479.3	20 896	383
504.8	19 812	361	470.6	21 248	352
495.8	20 170	360	463.0	21 598	350
		342			av 357 ± 13

[a] From a 20/1 solution of $\mathrm{Br^-/Mo_2}$.

$\times 10^{-3}$ M $\mathrm{Mo_2(O_2CCF_3)_4}$ in the presence of 20 equiv of $\mathrm{Br^-}$ is shown in Figure 1. After 15 min, two weak bands are observed: one centered at ~22 000 cm^{-1} and the other at ~19 000 cm^{-1}. In the crystal spectra of the diadducts the lowest observed transition was at ~22 000 cm^{-1}. This band in solution must correspond to this compound. However, after 36 h there was a great increase in the intensity of the band at 19 000 cm^{-1}, and the band at 22 000 cm^{-1} could no longer be seen. Intense vibrational structure was observed on the band at 19 000 cm^{-1}. The energies of the vibrational components, given in Table II, show a mean separation of 357 ± 13 cm^{-1}. This spacing suggests that this transition is not associated with the dibromo adduct. Raman data for this adduct indicated that the ground-state Mo–Mo stretch occurs at 366 cm^{-1}.[7] Moreover, this electronic transition is clearly metal localized and on the basis of the observed frequency is assigned as the $\delta \rightarrow \delta^*$ transition. Since such a transition will reduce the metal–metal bond order by 1, a substantial drop in the vibrational frequency should occur. If the excited-state frequencies of 357 ± 13 cm^{-1} were attributed to the same species that has a ground-state frequency of 366 cm^{-1}, a drop of only 9 ± 13 cm^{-1} would be implied, and this is too small. For example, the mean frequency observed in crystal of the bis(pyridine)adduct $\mathrm{[Mo_2(O_2CCF_3)_4(C_5H_5N)_2]}$ was 331 ± 9 cm^{-1} as compared to 397 cm^{-1} in the $\mathrm{Mo_2(O_2CCF_3)_4}$ molecule itself.[4]

We therefore consider two other possibilities as to the nature of the orange species in solution. One is that it is $\mathrm{[Mo_2(O_2CCF_3)_2Br_4]^{2-}}$. The low-temperature electronic spectrum of the compound $\mathrm{[Mo_2(O_2CCF_3)_2Cl_4]^{2-}}$ has been reported.[15] The 0–0 band was at 19 367 cm^{-1}, and the mean vibrational spacing was 354 ± 9 cm^{-1}, which is close to the value we have observed in the bromide solution. In addition, Garner and Senior reported that the conductivity of the orange solutions of the dibromo adduct in $\mathrm{CH_2Cl_2}$ was typical of 2:1 electrolytes.[7] This would be the case whether the diadduct or $\mathrm{[Mo_2(O_2CCF_3)_2X_4]^{2-}}$ was the species in solution. Lastly, since the tetrabromo species was actually isolated from this reaction, it appears likely it is present in the orange solution. However, the possibility of monodentate trifluoroacetates and bromides both being the ligands in the equatorial coordination plane cannot be completely ruled out. Such species have been observed in ligand-exchange reactions involving phosphines.[16] In any case, it is important to note that during recrystallization the predominant species in solution was not the compound in the resulting crystal. In fact, large amounts of amorphous orange solid were also obtained from crystallizations of both the dibromo and diiodo adducts.

The solutions of $\mathrm{[Mo_2(O_2CCF_3)_4]}$ and halide ion in acetone were quite similar in behavior to the previously reported reactions of $\mathrm{Mo_2(O_2CCF_3)_4}$ in pyridine.[6] Upon dissolution in pyridine, a bright red solution was produced, which displayed an absorption maximum at ~19 000 cm^{-1}. Upon cooling, this material became a gel. After the gel was washed with pentane, a yellow-orange powder was obtained, which was crystallized to obtain the bis(pyridine) adduct. The crystal spectrum of this product displayed little absorption in the region around 19 000 cm^{-1}. However, a band centered at 22 000 cm^{-1} was observed, which was assigned to the $\delta \rightarrow \delta^*$ transition.[4]

Table III. Positional Parameters and Their Estimated Standard Deviations in $\mathrm{(N\text{-}}n\mathrm{\text{-}Bu_4)_2[Mo_2(O_2CCF_3)_4Br_2]}$

atom	*x*	*y*	*z*
Mo1	−0.04449 (8)	0.0038 (1)	0.0569 (1)
Br	−0.1616 (1)	0.166 (1)	0.2141 (2)
F1	−0.1760 (8)	−0.263 (1)	−0.098 (1)
F2	−0.0729 (10)	−0.29 (1)	−0.164 (2)
F3	−0.1484 (12)	−0.216 (1)	−0.226 (2)
F4	−0.1230 (10)	0.219 (1)	−0.264 (1)
F5	−0.2168 (9)	0.182 (1)	−0.186 (1)
F6	−0.1820 (12)	0.103 (1)	−0.306 (2)
O1	−0.1036 (7)	0.1145 (7)	−0.0099 (9)
O2	0.0093 (6)	0.1235 (7)	0.1286 (8)
O3	−0.1232 (7)	0.0827 (8)	−0.0504 (9)
O4	0.0325 (7)	−0.0753 (8)	0.1732 (8)
N	−0.1717 (9)	0.2904 (9)	0.339 (1)
C2	−0.114 (1)	−0.240 (2)	−0.123 (2)
C4	−0.152 (1)	0.149 (2)	−0.233 (2)
C1	−0.073 (1)	−0.151 (1)	−0.086 (1)
C3	−0.098 (1)	0.098 (1)	−0.136 (1)
C5	−0.148 (2)	0.284 (2)	0.219 (2)
C6	−0.188 (2)	0.353 (2)	0.146 (2)
C7	−0.152 (2)	0.350 (2)	0.036 (3)
C8	−0.173 (3)	0.431 (4)	−0.017 (4)
C9	−0.267 (2)	0.279 (2)	0.339 (2)
C10	−0.309 (1)	0.206 (2)	0.280 (2)
C11	−0.395 (2)	0.204 (2)	0.295 (3)
C12	−0.445 (2)	0.136 (3)	0.233 (3)
C13	−0.144 (1)	0.385 (2)	0.393 (2)
C14	−0.153 (1)	0.395 (2)	0.504 (2)
C15	−0.137 (2)	0.497 (2)	0.535 (3)
C16	−0.129 (2)	0.524 (3)	0.637 (3)
C17	−0.130 (1)	0.213 (2)	0.405 (2)
C18	−0.045 (1)	0.217 (2)	0.413 (2)
C19	−0.011 (2)	0.135 (2)	0.491 (2)
C20	0.079 (2)	0.128 (2)	0.494 (3)

Solutions of $\mathrm{Mo_2(O_2CCF_3)_4}$ and halide ion in benzene behaved quite differently. In this case the orange color change was never observed. Instead, after the solution was refluxed, a yellow powder was produced. The electronic spectrum of this powder displayed an absorption at 22 000 cm^{-1} and was identical with the observed crystal spectrum of the dibromo adducts. However, benzene appears to be unique since in all other solvents tried the solutions were orange. Even washing the precipitate obtained from benzene with pentane turned the powder orange. When this precipitate was dissolved in acetone, an orange solution whose spectrum was identical with that of a solution of $\mathrm{[Mo_2(O_2CCF_3)_4]}$ and bromide ion resulted. All these observations suggest that the yellow powder obtained from benzene was $\mathrm{(N\text{-}}n\mathrm{\text{-}Bu_4)_2[Mo_2(O_2CCF_3)_4Br_2]}$. When a concentrated solution in benzene of the $\mathrm{[Mo_2(O_2CCF_3)_4]}$ and excess halide was made and not refluxed, it became a gel after several weeks. Addition of acetone resulted in two distinct phases, which were immiscible. Upon prolonged standing, large octahedral-shaped crystals of $\mathrm{(N\text{-}}n\mathrm{\text{-}Bu_4)_2[Mo_2(O_2CCF_3)_2X_4]}$ were obtained.

Attempts to duplicate these reactions using chloride ion were unsuccessful. Addition of chloride to acetone solutions of $\mathrm{Mo_2(O_2CCF_3)_4}$ did lead to an orange solution, but the rate of color change was much slower than for the other halides. Evaporation of these solutions produced only amorphous orange solids. These results are in agreement with those of Garner and Senior,[7] who reported that either the monoadduct or the compound $\mathrm{[Mo_2(O_2CCF_3)_3Cl_3]^{2-}}$ was obtained from such reactions.

Crystallography. The positional parameters and their errors for $\mathrm{(N\text{-}}n\mathrm{\text{-}Bu_4)_2[Mo_2(O_2CCF_3)_4Br_2]}$, $\mathrm{(N\text{-}}n\mathrm{\text{-}Bu_4)_2[Mo_2}$-

---

(15) Garner, C. D.; Parkes, S.; Walton, I. B.; Clegg, W. *Inorg. Chim. Acta* **1978**, *31*, L451.

(16) Girolami, G. S.; Mainz, V. V.; Andersen, R. A. *Inorg. Chem.* **1980**, *19*, 805.

Table IV. Position Parameters and Their Estimated Standard Deviations in $(N\text{-}n\text{-}Bu_4)_2[Mo_2(O_2CCF_3)_4I_2]$

atom	*x*	*y*	*z*	atom	*x*	*y*	*z*
Mo1	0.43844 (6)	0.47956 (5)	0.53319 (6)	N2	0.0242 (6)	0.3377 (4)	0.2729 (6)
Mo2	0.06355 (7)	0.02814 (5)	0.01510 (7)	C111	0.5202 (9)	0.0711 (6)	0.6591 (9)
I1	0.25085 (5)	0.41565 (4)	0.61619 (6)	C112	0.6303 (9)	0.0545 (7)	0.6992 (9)
I2	0.25477 (5)	0.10920 (4)	0.06665 (6)	C113	0.6928 (10)	0.0217 (7)	0.599 (1)
F11	0.377 (1)	0.3953 (9)	0.1736 (9)	C114	0.195 (1)	−0.0064 (10)	0.368 (1)
F12	0.7153 (10)	0.494 (1)	0.8148 (8)	C121	0.4494 (9)	0.0331 (7)	0.8284 (9)
F13	0.4206 (8)	0.4911 (7)	0.1208 (7)	C122	0.571 (1)	0.0470 (9)	0.224 (1)
F14	0.7551 (7)	0.2538 (4)	0.4535 (10)	C123	0.573 (1)	0.100 (1)	0.114 (1)
F15	0.6248 (8)	0.2142 (5)	0.451 (1)	C124	0.589 (2)	0.180 (2)	0.141 (2)
F16	0.688 (1)	0.2415 (7)	0.587 (1)	C131	0.3425 (10)	0.1181 (7)	0.6860 (10)
F21	0.938 (1)	0.1270 (7)	0.3522 (10)	C132	0.253 (1)	0.1460 (9)	0.755 (1)
F22	0.8148 (9)	0.067 (1)	0.3239 (9)	C133	0.157 (2)	0.166 (1)	0.659 (2)
F23	0.940 (1)	0.019 (1)	0.371 (1)	C134	0.077 (2)	0.182 (2)	0.710 (2)
F24	0.8701 (8)	0.2748 (5)	0.9010 (10)	C141	0.4716 (8)	0.1694 (7)	0.8162 (9)
F25	0.7421 (9)	0.2282 (7)	0.902 (1)	C142	0.4655 (10)	0.2441 (7)	0.751 (1)
F26	0.832 (1)	0.2079 (6)	0.7767 (9)	C143	0.500 (1)	0.3137 (9)	0.827 (1)
O11	0.4977 (5)	0.4950 (4)	0.6884 (5)	C144	0.424 (1)	0.3453 (10)	0.903 (1)
O12	0.3748 (5)	0.4615 (4)	0.3804 (5)	C211	0.0030 (7)	0.3910 (6)	0.3725 (8)
O13	0.5204 (5)	0.3601 (3)	0.5301 (5)	C212	0.9541 (9)	0.3536 (7)	0.4599 (9)
O14	0.6494 (5)	0.4018 (4)	0.4590 (5)	C213	0.9429 (9)	0.4122 (7)	0.5559 (9)
O21	0.1190 (5)	−0.0080 (4)	0.8622 (5)	C214	0.892 (1)	0.3824 (8)	0.648 (1)
O22	0.0141 (5)	0.0686 (4)	0.1679 (5)	C221	0.9329 (8)	0.3063 (6)	0.2314 (9)
O23	−0.0171 (6)	0.1372 (4)	0.9555 (5)	C222	0.8455 (9)	0.3748 (7)	0.1967 (10)
O24	0.8485 (5)	0.0791 (4)	0.9224 (5)	C223	0.752 (1)	0.3342 (9)	0.169 (1)
C11	0.4196 (8)	0.4791 (6)	0.3062 (8)	C224	0.669 (1)	0.3960 (10)	0.115 (1)
C12	0.375 (1)	0.468 (1)	0.198 (1)	C231	0.0619 (8)	0.3896 (6)	0.1924 (9)
C13	0.6075 (8)	0.3490 (6)	0.4926 (8)	C232	0.0808 (9)	0.3463 (7)	0.0851 (10)
C14	0.667 (1)	0.2652 (7)	0.489 (1)	C233	0.123 (1)	0.4055 (9)	0.014 (1)
C21	0.9328 (9)	0.0482 (7)	0.1955 (8)	C234	0.121 (1)	0.376 (1)	0.899 (2)
C22	0.893 (2)	0.084 (2)	0.296 (1)	C241	0.1062 (8)	0.2606 (6)	0.2976 (8)
C23	0.8938 (10)	0.1358 (7)	0.9217 (8)	C242	0.2101 (9)	0.2813 (6)	0.3283 (9)
C24	0.836 (1)	0.2131 (9)	0.876 (1)	C243	0.2785 (9)	0.2020 (7)	0.3707 (9)
N1	0.4446 (6)	0.0979 (5)	0.7483 (7)	C244	0.384 (1)	0.2166 (8)	0.402 (1)

Table V. Positional Parameters and Their Estimated Standard Deviations for $(N\text{-}n\text{-}Bu_4)_2[Mo_2(O_2CCF_3)_2Br_4]$

atom	*x*	*y*	*z*
Mo1	0.46839 (6)	0.44116 (4)	0.47548 (5)
Br1	0.29695 (7)	0.46330 (7)	0.36061 (8)
Br2	0.59004 (9)	0.32193 (6)	0.54351 (7)
F1	0.5966 (6)	0.4603 (5)	0.1794 (5)
F2	0.3881 (6)	0.4110 (5)	0.7981 (5)
F3	0.2729 (5)	0.4885 (7)	0.7353 (5)
O1	0.3975 (5)	0.4295 (3)	0.6005 (4)
O2	0.5335 (4)	0.4440 (3)	0.3468 (4)
N1	0.4316 (6)	0.1927 (5)	0.2458 (5)
C1	0.4158 (7)	0.4896 (6)	0.6628 (6)
C2	0.3688 (8)	0.4827 (7)	0.7531 (6)
C11	0.5367 (7)	0.2345 (6)	0.2812 (7)
C12	0.6092 (8)	0.2260 (7)	0.2075 (7)
C13	0.7143 (8)	0.2568 (8)	0.2648 (9)
C14	0.7864 (10)	0.2678 (10)	0.1944 (11)
C21	0.3790 (8)	0.2259 (6)	0.1457 (6)
C22	0.3605 (9)	0.3215 (7)	0.1424 (7)
C23	0.3181 (10)	0.3473 (8)	0.0360 (8)
C24	0.2934 (12)	0.4427 (8)	0.0283 (11)
C31	0.3716 (7)	0.2142 (6)	0.3287 (6)
C32	0.2642 (8)	0.1796 (8)	0.3093 (7)
C33	0.2171 (9)	0.2070 (9)	0.3933 (9)
C34	0.1042 (11)	0.1856 (10)	0.3774 (11)
C41	0.4390 (8)	0.0973 (5)	0.2333 (6)
C42	0.4849 (11)	0.0502 (6)	0.3272 (9)
C43	0.4916 (11)	−0.0466 (6)	0.3037 (9)
C44	0.5156 (13)	−0.0973 (9)	0.3880 (11)

$(O_2CCF_3)_4I_2]$, and $(N\text{-}n\text{-}Bu_4)_2[Mo_2(O_2CCF_3)_2Br_4]$ are given in Tables III, IV, and V, respectively. The bond distances and angles for the anions $[Mo_2(O_2CCF_3)_4X_2]^{2-}$ (X = Br, I) are given in Table VI and for $[Mo_2(O_2CCF_3)_2Br_4]^{2-}$ in Table VII. The numbering scheme used for the diadducts is essentially the same. In the case of the diiodo adduct there were two independent molecules, whose labels include an additional leading digit of 1 or 2. ORTEP diagrams illustrating the numbering schemes are shown in Figures 2 and 3.

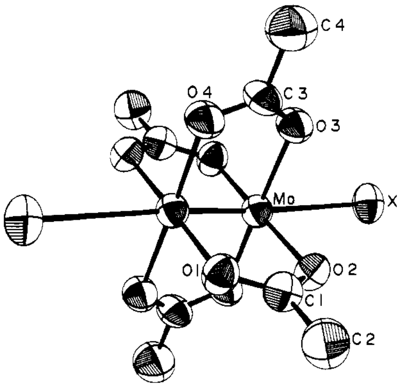

Figure 2. ORTEP drawing of $[Mo_2(O_2CCF_3)_4X_2]^{2-}$ illustrating the numbering scheme used. The drawing is of molecule 1 of the diiodo adduct. The thermal ellipsoids are of 50% probability. Fluorine atoms have been omitted for clarity.

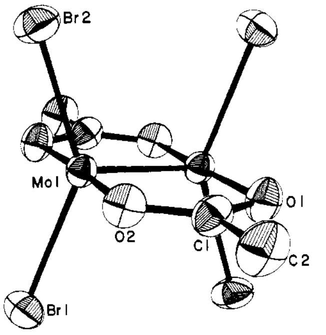

Figure 3. View of $[Mo_2(O_2CCF_3)_2Br_4]$. Fluorine atoms have been omitted for clarity.

The most surprising result of the structural studies is that the diiodo and dibromo adducts of $[Mo_2(O_2CCF_3)_4]$ are not isostructural. The dibromo adduct crystallized in the monoclinic space group $P2_1/n$. Since there were only two molecules

Table VI. Bond Distances (Å) and Angles (deg) for $[Mo_2(O_2CCF_3)_4X_2]^{2-}$

	X = Br	X = I	
	Mo	Mo1	Mo2
Mo-Mo	2.134 (2)	2.140 (2)	2.136 (2)
Mo-O1	2.109 (9)	2.110 (6)	2.123 (6)
-O2	2.115 (8)	2.113 (6)	2.111 (7)
-O3	2.093 (10)	2.110 (6)	2.107 (7)
-O4	2.147 (9)	2.127 (6)	2.131 (7)
-X	2.879 (3)	3.180 (1)	3.187 (1)
O1-C1	1.24 (2)	1.28 (1)	1.26 (1)
O2-C1	1.28 (2)	1.22 (1)	1.28 (1)
C1-C2	1.51 (3)	1.49 (2)	1.46 (2)
C2-F1	1.15 (3)	1.26 (2)	1.21 (2)
-F2	1.16 (3)	1.27 (2)	1.23 (2)
-F3	1.38 (4)	1.29 (2)	1.46 (2)
O3-C3	1.19 (2)	1.25 (1)	1.26 (1)
O4-C3	1.26 (2)	1.26 (1)	1.24 (1)
C3-C4	1.60 (4)	1.49 (1)	1.51 (2)
C4-F4	1.21 (3)	1.26 (1)	1.25 (1)
-F5	1.35 (3)	1.20 (1)	1.30 (2)
-F6	1.18 (4)	1.33 (2)	1.26 (2)
Mo'-Mo-O1[a]	91.2 (3)	91.3 (2)	91.5 (2)
-O2	91.9 (3)	91.0 (2)	91.7 (2)
-O3	91.9 (3)	91.3 (2)	91.7 (2)
-O4	90.9 (3)	91.5 (2)	91.3 (2)
-X	178.6 (1)	176.17 (6)	178.25 (6)
O1-Mo-O2	176.9 (4)	177.6 (3)	176.8 (3)
-O3	89.0 (4)	88.8 (2)	90.2 (2)
-O4	91.4 (2)	90.6 (2)	90.0 (3)
-X	90.2 (2)	92.5 (2)	89.6 (2)
O2-Mo-O3	90.3 (4)	90.7 (2)	89.0 (3)
-O4	89.1 (4)	89.8 (2)	90.7 (3)
-X	86.8 (2)	85.2 (2)	87.3 (2)
O3-Mo-O4	177.2 (4)	177.2 (2)	177.0 (3)
-X	88.7 (2)	88.3 (2)	89.7 (2)
O4-Mo-X	88.5 (2)	89.0 (2)	87.3 (2)
Mo-O1-C1	116 (1)	114.8 (6)	116.0 (6)
-O2-C1	114 (1)	116.4 (6)	115.9 (6)
O1-C1-O2	126 (2)	126.5 (9)	124.9 (9)
-C2	113 (2)	116 (1)	119 (1)
O2-C1-C2	120 (2)	117 (1)	116 (1)
C1-C2-F1	124 (2)	112 (2)	121 (1)
-F2	115 (2)	114 (1)	118 (1)
-F3	101 (4)	116 (1)	101 (2)
F1-C2-F2	119 (4)	108 (2)	121 (1)
-F3	92 (3)	103 (1)	85 (2)
F2-C2-F3	88 (3)	103 (2)	83 (2)
Mo-O3-C3	114 (1)	115.8 (6)	114.9 (7)
-O4-C3	111 (1)	115.0 (6)	114.5 (7)
O3-C3-O4	132 (2)	126.3 (9)	128 (1)
-C4	122 (2)	117 (1)	115 (1)
O4-C3-C4	106 (2)	117 (1)	117 (1)
C3-C4-F4	115 (3)	117 (1)	116 (1)
-F5	104 (3)	117 (1)	112 (1)
-F6	116 (3)	108 (1)	111 (1)
F4-C4-F5	101 (3)	108 (1)	107 (1)
-F6	113 (4)	100 (1)	106 (2)
F5-C4-F6	105 (3)	102 (1)	104 (1)

[a] Atoms with a prime are related by a center of inversion in this and all other tables.

Table VII. Bond Distances (Å) and Bond Angles (deg) for $(N\text{-}n\text{-}Bu_4)_2[Mo_2(O_2CCF_3)_2Br_4]$

Mo1-Mo1'	2.098 (1)	Mo1-Br2	2.545 (1)
Mo1-Br1	2.542 (1)	Mo1-O2	2.114 (4)
Mo1-O1	2.122 (4)	O2-C1	1.269 (8)
O1-C1	1.269 (8)		
C1-C2	1.50 (1)		
C2-F1	1.31 (1)		
-F2	1.29 (1)		
-F3	1.26 (1)		
Mo1'-Mo1-Br1	109.64 (4)	Mo1'-Mo1-Br2	110.39 (4)
-O1	91.9 (1)	-O2	92.5 (1)
Br1-Mo1-O1	91.2 (1)	Br2-Mo1-O1	89.7 (1)
-O2	87.0 (1)	-O2	89.1 (1)
O1-Mo1-O2	175.6 (2)	Br1-Mo1-Br2	139.90 (3)
Mo1-O1-C1	114.9 (4)	Mo1-O2-C1	114.8 (4)
O1-C1-C2	116.4 (7)	O2-C1-C2	117.7 (7)
C1-C2-F1	112.8 (8)		
-F2	112.5 (8)		
-F3	114.1 (8)		
F1-C2-F2	104.8 (8)		
-F3	107.0 (9)		
F2-C2-F3	104.9 (9)		

in the cell, they must be located about a center of inversion. The inversion centers used were at (0, 0, 0) and ($^1/_2$, $^1/_2$, $^1/_2$). The diiodo adduct crystallized in the triclinic space group $P\bar{1}$. However, if the *a* and *b* axes are interchanged, the cells are fairly similar. The greatest difference was in the angle between the *a* and *b* axes, which was 90° for the bromide but only 78.48 (1)° for the iodide. The packing in the iodide was also similar to that of the bromide. Again there were two molecules within the unit cell. However, instead of single molecules situated on general positions with inversion centers between them, it was found that each of two independent molecules resided on the inversion centers located at (0, 0, 0) and ($^1/_2$, $^1/_2$, $^1/_2$). However, there was a consequence of the lower cell symmetry. In the dibromo adduct, the two molecules are related by a glide plane and a screw axis. These operations were almost entirely translational because the Mo–Mo bond lay approximately in the *xz* plane. In fact, the Mo–Mo vectors of the two anions made an angle of 174° with respect to each other. In the triclinic cell the two anions were not related by any symmetry operation. In this case the observed angle was 146°.

The second surprising aspect of these structures was that the molar volume of the diiodo adduct was smaller than that of the analogous bromide. In view of the significantly longer distance for the Mo–I bond as compared to the Mo–Br bond, this was not expected. The fact that the iodide compounds occupy a smaller volume suggests that for the bromo compound crystallization has not produced the most efficient packing. One reason for this may be that the crystals were obtained from a solution in which there is an equilibrium between the compound crystallizing and another species. The fact that $(N\text{-}n\text{-}Bu_4)_2[Mo_2(O_2CCF_3)_2Br_4]$ also crystallized in a similar cell (space group $P2_1/n$; $Z = 2$) may provide some support for this theory.

The structure of the individual anions were as expected. All are based on an essentially square-planar arrangement of ligands in the equatorial coordination plane. The only large deviation was the Mo–Mo–Br angle of ~110° in $[Mo_2(O_2CCF_3)_2Br_4]^{2-}$. However, this increase from 90° is typical and arises because twice the Br^- van der Waals radius is greater than the Mo–Mo distance. The observed angle was slightly larger than the 106.29 (8)° observed in $[Mo_2Br_8]^{4-}$.[17] This can be attributed to the shorter Mo–Mo distance of 2.098 (1) Å in $[Mo_2(O_2CCF_3)_2Br_4]^{2-}$ as compared to 2.130 (4) Å in $[Mo_2Br_8]^{4-}$. All of the distances and angles involving molybdenum and the trifluoroacetate ligands were typical.

The Mo–Mo distances displayed an interesting variation. The metal–metal distance in $Mo_2(O_2CCF_3)_4$ was 2.090 (4) Å.[5] The substitution of four bromide ions for two trifluoroacetate ligands lengthens the bond only slightly, to 2.098 (1) Å. However, in view of the large esd in the Mo–Mo bond length in $Mo_2(O_2CCF_3)_4$, this increase is within three standard deviations and may not be real. The Mo–Mo bond distances in the diadducts were much longer at 2.134 (2), 2.140 (2), and 2.136 (2) Å for the bromide and two independent iodide adduct anions. These distances were longer than the 2.129 (2) Å reported for the bis(pyridine) adduct.[6] On the other hand, the Mo–X distances are also quite long, indicating only weak

---

(17) Brencic, J. V.; Leban, I.; Segedin, P. *Z. Anorg. Allg. Chem.* **1976**, *427*, 85.

axial coordination. The Mo–Br distance of 2.879 (3) Å was substantially longer than the 2.604 (1) Å distance in $[Mo_2Br_8]^{4-}$[16] or the 2.542 (1) and 2.545 (1) Å distances in $[Mo_2(O_2CCF_3)_2Br_4]^{2-}$. Similarly the Mo–I bonds at 3.180 (1) and 3.187 (1) Å were much longer than the ~2.78 Å observed in $[Mo_2I_6(H_2O)_2]^{2-}$.[18] This is in agreement with the very long Mo–N distance reported in the bis(pyridine) adduct.

The fluorine atoms in all the compounds reported were very anisotropic with extremely large temperature parameters. For this reason they have been omitted from Figures 2 and 3. This behavior, which is not uncommon for fluorine atoms on trifluoromethyl groups, can be attributed to rotation about the C–C bond resulting in the large thermal ellipsoids. This motion also resulted in large variations and errors in the C–F bond lenghts and C–C–F bond angles.

Registry No. $(N(n\text{-}Bu)_4)_2[Mo_2(O_2CCF_3)_4Br_2]$, 84987-30-4; $(N(n\text{-}Bu)_4)_2[Mo_2(O_2CCF_3)_4I_2]$, 84987-31-5; $(N(n\text{-}Bu)_4)_2[Mo_2(O_2CCF_3)_2Br_4]$, 7439-98-7.

Supplementary Material Available: Listings of bond distances and angles for the tetrabutylammonium cations (Table VIII), thermal parameters and their errors (Tables IX, X, and XI), and observed and calculated structure factors (Tables XII, XIII, and XIV) (59 pages). Ordering information is given on any current masthead page.

---

(18) (a) Brencic, J. V.; Segedin, P. *Inorg. Chim. Acta* **1978**, *29*, L287. (b) Brencic, J. V.; Golic, L. *J. Cryst. Mol. Struct.* **1977**, *7*, 183.

Contribution from the Department of Chemistry, University of Cincinnati, Cincinnati, Ohio 45221,
and the Miami Valley Laboratories, Procter & Gamble Company, Cincinnati, Ohio 45239

Calcium Affinity of Coordinated Diphosphonate Ligands. Single-Crystal Structure of $[(en)_2Co(O_2P(OH)CH_2P(OH)O_2)]ClO_4\cdot H_2O$. Implications for the Chemistry of Technetium-99m-Diphosphonate Skeletal Imaging Agents

SILVIA S. JURISSON,[1] JAMES J. BENEDICT,[2] R. C. ELDER,[1] R. WHITTLE,[1] and EDWARD DEUTSCH*[1]

Received August 2, 1982

A series of (diphosphonato)bis(ethylenediamine)cobalt(III) complexes, where the diphosphonate ligand has the formula $HO_3P\text{–}CR(R')\text{–}PO_3H^{2-}$, has been prepared. Members of the series include the following R/R′ combinations: H/H, H/CH_3, CH_3/CH_3, H/OH, CH_3/OH, phenyl/OH, *tert*-butyl/OH, H/NH_2, CH_3/NH_2, H/$N(CH_3)_2$, H/Cl, and Cl/Cl. The complexes have been characterized in all cases by visible–UV, IR, ^1H NMR, and ^{31}P NMR spectra, in several cases by elemental analyses, and for the prototype title complex (R/R′ = H/H) by single-crystal X-ray structural analysis refined to a conventional R factor of 0.034. Equilibrium constants governing the one-to-one association with calcium(II) in dilute aqueous solution (pH 10, NH_4OH/NH_4Cl buffer, $\mu = 0.1$ M (KCl), 25 °C) have been determined potentiometrically for all diphosphonate complexes as well as for the analogous pyrophosphato and oxalato complexes. Values of the equilibrium constants for the H/OH, H/H, and CH_3/OH complexes are 2.4×10^6, 1.8×10^4, and 1.1×10^4 M^{-1}, respectively, showing (a) that coordinated diphosphonate ligands have considerable affinity for calcium(II) and (b) that when R′ = OH the calcium affinity is enhanced, presumably via coordination of this OH group to calcium and formation of a bidentate–tridentate bridge from cobalt to calcium. This ordering of affinities exactly parallels the ordering of skeletal uptake of these three diphosphonate ligands when labeled with ^{99m}Tc, implying that binding of Tc–diphosphonate complexes to calcium at the surface of bone is an important step in the mechanism of in vivo action of ^{99m}Tc–diphosphonate skeletal imaging agents.

Introduction

Diphosphonates are a class of ligands that are chemically related to, and mimic the physiological behavior of, pyrophosphate:

$$\underset{\text{pyrophosphate}}{O_3P\text{–}O\text{–}PO_3^{4-}} \qquad \underset{\text{diphosphonate}}{O_3P\text{–}CR(R')\text{–}PO_3^{4-}}$$

Most importantly, both pyrophosphate and diphosphonate ligands have very high affinity for calcium(II) in homogeneous solution and at the surfaces of minerals and bone. However, for many physiological applications diphosphonates are superior to pyrophosphate in that (1) the P–CR(R′)–P linkage is much more resistant to hydrolysis than is the P–O–P linkage[3] and (2) by variation of the R and R′ groups of the diphosphonate backbone the chemical and biological properties of these ligands can be extensively modified. Simple diphosphonate salts are used therapeutically for the treatment of bone and calcium metabolic disorders,[4] but more importantly, diphosphonate complexes of technetium-99m are widely used as diagnostic agents.[5] These agents are referred to as radiopharmaceuticals because it is the γ-ray activity of the ^{99m}Tc that provides the diagnostic image.[6] ^{99m}Tc–diphosphonate radiopharmaceuticals accumulate at sites of high calcium metabolic activity such as those that occur in the skeleton or in areas of recently infarcted myocardium.[7] Very little is known about the in vivo mechanism of action of these clinically important agents, but it is generally thought to be the residual chemical affinity of the *coordinated* diphosphonate ligand of the technetium–diphosphonate complex that drives deposition of the radiopharmaceutical at sites of high calcium metabolic activity.[8] For this reason we sought to investigate the calcium affinity of *coordinated* diphosphonate (and pyrophosphate) ligands and especially to determine how calcium affinity varies with the nature of the R and R′ substituent groups. Also of interest is whether or not these chemical

---

(1) University of Cincinnati.
(2) Procter & Gamble Co.
(3) Francis, M. D.; Centner, R. L. *J. Chem. Educ.* **1978** *55*, 760–6.
(4) Khairi, M. A. A.; Meunier, P.; Edouard, C.; et al. *Calcif. Tissue Res.* **1977**, *22*, 355–8 (suppl.).
(5) (a) Tofe, A. J.; Francis, M. D. *J. Nucl. Med.* **1974**, *15*, 69–74. (b) Eckelman, W. C.; Levenson, S. M. *Int. J. Appl. Radiat. Isot.* **1977**, 28, 67–82. (c) Jones, A.; Francis, M. D.; Davis, M. A. *Semin. Nucl. Med.* **1976**, *6*, 3–18.
(6) Hayes, R. L. "The Chemistry of Radiopharmaceuticals"; Heindel, N. D.; Burns, H. D., Honda, T., Brady, L. W., Eds.; Masson: New York, 1978; pp 155–68.
(7) Francis, M. D.; Slough, C. L.; Tofe, A. J. *Calcif. Tissue Res.* **1976**, *20*, 303.
(8) Deutsch, E. "Radiopharmaceuticals II: Proceedings of the Second International Symposium on Radiopharmaceuticals"; Society of Nuclear Medicine: New York, 1979; pp 129–46.